

Hyaluronan-CD44-ERK1/2 Regulate Human Aortic Smooth Muscle Cell Motility during Aging*

Received for publication, November 5, 2007, and in revised form, December 12, 2007. Published, JBC Papers in Press, December 12, 2007, DOI 10.1074/jbc.M709051200

Davide Vigetti[‡], Manuela Viola[‡], Eugenia Karousou[‡], Manuela Rizzi[‡], Paola Moretto[‡], Anna Genasetti[‡], Moira Clerici[‡], Vincent C. Hascall[§], Giancarlo De Luca^{‡1}, and Alberto Passi^{‡1}

From the [‡]Dip. di Scienze Biomediche Sperimentali e Cliniche, Università degli Studi dell'Insubria, via J. H. Dunant 5, 21100 Varese, Italy and the [§]Department of Biomedical Engineering and Orthopaedic Research Center/ND20, The Cleveland Clinic Foundation, Cleveland, Ohio 44195

The glycosaminoglycan hyaluronan (HA) modulates cell proliferation and migration, and it is involved in several human vascular pathologies including atherosclerosis and vascular restenosis. During intima layer thickening, HA increases dramatically in the neointima extracellular matrix. Aging is one of the major risk factors for the insurgence of vascular diseases, in which smooth muscle cells (SMCs) play a role by determining neointima formation through their migration and proliferation. Therefore, we established an *in vitro* aging model consisting of sequential passages of human aortic smooth muscle cells (AoSMCs). Comparing young and aged cells, we found that, during the aging process *in vitro*, HA synthesis significantly increases, as do HA synthetic enzymes (*i.e.* HAS2 and HAS3), the precursor synthetic enzyme (UDP-glucose dehydrogenase), and the HA receptor CD44. In aged cells, we also observed increased CD44 signaling that consisted of higher levels of phosphorylated MAP kinase ERK1/2. Further, aged AoSMCs migrated faster than young cells, and such migration could be modulated by HA, which alters the ERK1/2 phosphorylation. HA oligosaccharides of 6.8 kDa and an anti-CD44 blocking antibody prevented ERK1/2 phosphorylation and inhibited AoSMCs migration. These results indicate that, during aging, HA can modulate cell migration involving CD44-mediated signaling through ERK1/2. These data suggest that age-related HA accumulation could promote SMC migration and intima thickening during vascular neointima formation.

Hyaluronan (HA)² is a linear, unsulfated glycosaminoglycan (GAG) that is composed of repeating units of D-glucuronic acid

* This work was supported by Ministero dell'Università e della Ricerca (PRIN) (to D. V.), University of Insubria (FAR) (to D. V., A. P., M. V., and G. D. L.), and by Centro Interuniversitario di Biotecnologie (CIB) (to A. P.). The costs of publication of this article were defrayed in part by the payment of page charges. This article must therefore be hereby marked "advertisement" in accordance with 18 U.S.C. Section 1734 solely to indicate this fact.

¹ To whom correspondence should be addressed: Dipartimento di Scienze Biomediche Sperimentali e Cliniche, Università degli Studi dell'Insubria, via J. H. Dunant 5, 21100 Varese, Italy. Tel.: 39-0332-217142; Fax: 39-0332-217119; E-mail: alberto.passi@uninsubria.it.

² The abbreviations used are: HA, hyaluronan; GAG, glycosaminoglycan; RT-PCR, reverse transcriptase-polymerase chain reaction; HAS, HA synthase(s); HYAL, hyaluronidase(s); FACE, fluorophore-assisted carbohydrate electrophoresis; AMAC, 2-aminoacridone; HWH, high molecular weight HA; UGDH, UDP-glucose dehydrogenase; ΔCS-4S, chondroitin 4 sulfate disaccharide; ΔCS-6S, chondroitin 6 sulfate disaccharide; αSM actin, α-smooth muscle actin; AoSMCs, aortic smooth muscle cells; ERK, extracellular signal-regulated kinase; PBS, phosphate-buffered saline; FBS, fetal bovine serum; ECM, extracellular matrix.

and N-acetylglucosamine linked together through alternating β1,4 and β1,3 glycosidic bonds. The amount and the molecular weight of HA are important factors that regulate the physiopathological effects that this molecule displays on cells (1). In mammals, three specific HA synthases (HAS1, -2, and -3) and three hyaluronidases (HYAL1, 2, and PH20) regulate HA synthesis and degradation with specific biochemical properties and distributions in adult as well as in embryonic tissues (2, 3). Therefore, these enzymes have a critical role in HA metabolism and are responsible for HA balance in the extracellular matrix (ECM).

Hydrated HA makes the ECM an ideal environment in which cells can move and proliferate. Moreover, HA is an important space filling molecule as is evident in the vitreous humor, the dermis and the synovial fluid of joints. Besides its chemical and mechanical properties, HA interacts with several receptors at the cellular level that specifically trigger various signal transduction responses (4). The HA receptor CD44 is expressed on the surface of most cells, including immune system cells, and it mediates cell adhesion, proliferation and migration (5). Receptor for HA-mediated motility (RHAMM) mediates cellular motility (6). Lyve-1 is the specific HA receptor of the lymphatic system although very recent evidences indicate a more complex function of this protein unrelated to HA (7). HA Receptor for Endocytosis (HARE) mediates the endocytosis of HA (8, 9). Recently, Toll Like Receptors 4 and 2 (TLR4/2) were shown to recognize HA fragments (10) and modulate the inflammation response in the lung (11). Although it has a simple structure, it is clear that HA can modulate many cellular responses, and the amount of this GAG has to be strictly regulated. Cells during different stress responses synthesize HA cable-like structures that have a role in inflammation, acting as an adherent for monocytes and other immune system cells (12–15). A large body of evidence describes a direct correlation between the amounts of HA and degree of malignancy in cancers. Considering the role of HA in cell proliferation and migration, the correlation between malignancy and HA content opened a new insight in tumor biology (16).

In vascular pathology, HA accumulates during the formation of neointima, which reduces the vessel diameter and is a crucial event for the pathological outcome (17). In the first steps of its formation, neointima tissue is composed mainly of proliferating smooth muscle cells (SMCs) that migrated from the tunica media of the vessel after a mechanical or other undefined injury. In this context, HA and CD44 have a pivotal role to

induce SMC proliferation and migration (18). Transgenic mice overexpressing HAS2 have high HA levels in the vasculature and developed more serious atherosclerotic lesions compared with controls (19). Moreover, in other experiments, CD44 knock-out mice showed slower SMC proliferation rates than control mice and less severe atherosclerotic lesions (5).

As aging is one of the major risk factors for the insurgen of vascular pathology (20), we have established a cell model for *in vitro* aging in order to investigate age related modifications in gene expression and cellular migration in primary human aortic SMCs (AoSMCs). Recently, we used this aging model to describe age related changes in expression and activity of matrix metalloproteinase 2 (21). In this study, we describe the age-related changes in HA content, including the gene expression of enzymes involved in HA metabolism, and its effect on the migration properties of young and aged AoSMCs. The data obtained suggest that HA can regulate cell migration through a CD44 pathway that modulates ERK1/2 phosphorylation.

EXPERIMENTAL PROCEDURES

Cell Culture—Human primary aortic smooth muscle cells (AoSMCs, donor age 17, male) were purchased from Cambrex and grown in SmGm2 complete culture medium (Cambrex) supplemented with 5% fetal bovine serum (FBS). This cell culture medium was used in all the experiments. The cultures were maintained in an atmosphere of humidified 95% air, 5% CO₂ at 37 °C. Whenever cultures became nearly confluent, the cells were trypsinized, counted using trypan blue exclusion, and subcultured. Population doublings (PDs) were determined at each passage and were calculated as follows: PD = log (number of cells obtained/initial number of cells)/log 2. In the experiments, 4 PD and 18 PD cells were used and are referred to as young and aged AoSMCs, respectively.

HA Quantification—HA and chondroitin sulfate were quantified by means of fluorophore-assisted carbohydrate electrophoresis (FACE) and HPLC analysis (22). Briefly, GAGs were purified starting from 300 μ l of conditioned culture medium of young and aged AoSMCs by proteinase K (Fynzyme) digestion and ethanol precipitation. GAGs associated with the cell layer were analyzed by resuspending the AoSMCs in 0.1 M ammonium acetate, pH 7, disrupting the cells with sonication, digesting with proteinase K, and recovering the GAGs by ethanol precipitation. GAGs were digested with hyaluronidase SD (Seikagaku) and by chondroitinase ABC (Seikagaku). Disaccharides obtained by the enzymatic digestions were fluorotagged with 2-aminoacridone (AMAC, Molecular Probes). AMAC-tagged disaccharides were separated and quantified with FACE and HPLC.

Determination of HA Molecular Size—Gel filtration chromatography was done on AMAC derivatized GAGs purified from young and aged AoSMC conditioned culture media as previously described (23) using an FPLC (Amersham Biosciences) apparatus. Sample peaks were identified and quantified by comparing the absorbance at 280 nm with standard proteins. The identification and quantification of GAGs was done on eluted fractions (2 ml each) by digestion with hyaluronidase SD and chondroitinase ABC and analysis as described above.

HA Localization—Immunofluorescence experiments were done as previously described by de la Motte *et al.* (12). Briefly, young and aged AoSMCs grown on coverslips were fixed in cold methanol for 15 min. The coverslips were preincubated with PBS containing 2% FBS and then incubated in the same solution containing biotinylated HA-binding protein (Seikagaku) (5 μ g/ml) and a CD44 monoclonal antibody (clone A3D8, Sigma; 10 μ g/ml) overnight at 4 °C. The coverslips were washed with PBS, and then incubated with a solution containing fluorescein-tagged streptavidin (1:500) and Texas Red-conjugated anti-mouse Ig (H+L) (1:500) in PBS containing 2% FBS. After washing in PBS, the coverslips were mounted using mounting medium containing 4,6-diamidino-2-phenylindole (DAPI) (Vector Laboratories). The slides were then sealed with nail polish and images were obtained using a fluorescence microscope (Olympus).

Quantitative and Semiquantitative RT-PCR—Total RNA from both young and aged AoSMCs was extracted using TRIzol reagent (Invitrogen) following the manufacturer's protocol. Total RNA from human normal fetal aorta (Stratagene) and total RNA from human adult aorta (Ambion) were used to quantify the gene expression *in vivo*. To remove DNA contamination, DNase (Ambion) treatment was done in all samples. One μ g of total RNA was retrotranscribed using the High Capacity cDNA synthesis kit (Applied Biosystems) for 2 h at 37 °C. Quantitative RT-PCR was done on an Abi Prism 7000 instrument (Applied Biosystems) using Taqman Universal PCR Master Mix (Applied Biosystems) following the manufacturer's instructions. Probes and primers were from TaqMan gene expression assay reagents (Applied Biosystems). The following TaqMan gene expression assays were used: HAS1 (Hs00155410), HAS2 (Hs00193435), HAS3 (Hs00193436), HYAL2 (Hs00186841), PH20 (Hs00162139), smooth muscle α -actin (Hs00224622), ICAM (Hs00164932), VCAM (Hs00174239), CD44 (Hs00174139), RHAMM (Hs00234864), UDP-glucose dehydrogenase (UGDH) (Hs00163365) and RNaseP (Hs00706565_s1). Fluorescent signals generated during PCR amplifications were monitored and analyzed with Abi Prism 7000 SDS software (Applied Biosystems). Comparison of the amount of each gene transcript among different samples was made using RNaseP as the reference. In order to determine the efficiency of each Taqman gene expression assay, standard curves were generated by serial dilution of cDNA, and quantitative evaluations of target and housekeeping gene levels were obtained by measuring threshold cycle numbers (Ct). As the differences among efficiencies of each Taqman gene expression assay were <0.1, we used the relative quantification method $\Delta\Delta$ Cts to quantify gene expression (24).

The Taqman assay for HYAL1 detects mRNAs coding for both the active and the inactive splicing variants. Therefore, we designed two primers (5'-ACTTTCTAAGCCCCAACTA-CACC-3' and 5'-GGTTCTTGTATTTTCCAGCTC-3') to detect only the active HYAL1 wild-type transcript (25) in canonical semiquantitative RT-PCR experiments using RED-Taq (Sigma). Moreover, to detect HYAL3 we designed 5'-TGTCGCCAGGATGACCTTGTG-3' and 5'-TCTAC-CCCTCAGGGATTCCA-3'-specific primers, and to detect HYAL4 we designed 5'-GCGCCCAGTTACCTTCACTT-3'

Hyaluronan during Smooth Muscle Cell Aging

and 5'-GCAACTTAAATATTCCAATAAGGAGGA-3' primers. For standardization, β -actin was also amplified by using 5'-GGCACCCAGCACAATGAAG-3' and 5'-GCCGATCCACACGGAGTACT-3' primers.

Detection of Hyaluronidase Activity by Zymography—Cell lysates from young and aged AoSMC cultures were obtained by disrupting the cells with sonication in PBS with 0.1% Triton X-100. Medium samples were concentrated 10 \times in a filtration apparatus with a cut-off of 10,000 Da. Aliquots of these samples were electrophoresed in a 12% polyacrylamide gel containing 1 mg/ml of HA (26). The gel was rinsed for 2 h in 2.5% Triton X-100 and incubated overnight at 37 °C in 50 mM citric acid-Na₂HPO₄, 0.15 M NaCl, pH 5, or in 0.1 M sodium formate, 0.15 M NaCl, pH 3.5. Each gel was treated with 0.1 mg/ml Pronase in 20 mM Tris-HCl, pH 8.0 for 2 h at 37 °C and stained with Alcian Blue.

The electrophoretic assay of hyaluronidase activity was also used as described (27). Briefly, 50 μ g of HA from human umbilical cord (Sigma) was incubated with young or aged AoSMC-conditioned medium or with 30 μ g of cell lysate proteins prepared by exposing young or aged AoSMC cultures to a PBS buffer containing 0.5% Triton X-100. After incubation at 37 °C at pH 3.5 (using formate buffer, see above) or at pH 5 (using citric acid-Na₂HPO₄ buffer, see above), the samples were boiled and electrophoresed in standard 0.5% agarose Tris acetate-EDTA gels, and HA was stained with 0.005% Stains-All (Sigma).

Migration Assay—Cell migration was measured with the Transwell (Costar) system, which allows cells to migrate through 8- μ m pore size polycarbonate membranes as described previously (21). Briefly, 10⁵ cells were resuspended in serum-free SmGm2 and added to the upper chamber of Transwells. The lower chamber was filled with 1.5 ml serum-free SmGm2 or 1.5 ml serum-free SmGm2 containing 10 μ g/ml of purified, low endotoxin 34-mer HA oligosaccharide (28), or 10 μ g/ml of high molecular weight HA (Healon, Amersham Biosciences), or anti CD44 monoclonal antibodies (clone A3D8 at 15 μ g/ml or clone BRIC235 at 5 μ g/ml), or 15 μ g/ml of an isotype-matched control antibody against tubulin (clone DM1A, Sigma), or 15 μ M (final concentration) of U0126 (Sigma), or 10 ng/ml of PDGF-BB (Euroclone), or 20% FBS (Euroclone). In control experiments, HWHA was digested with 30 milliunits of chondroitinase ABC (Seikagaku) at 37 °C for 16 h to obtain HA disaccharides. After 6 h, filters were removed, and cells remaining on the upper surface of the membrane were removed with a cell scraper. The cells present beneath the membrane were fixed with cold methanol and stained with Crystal violet. Cells were counted in 10 high-power microscope fields.

Western Blotting—Young and aged AoSMC cultures were lysed in ice-cold PBS buffer containing 0.5% Triton X-100, and a phosphatase and protease inhibitor mixture (Roche Applied Science) by means of sonication. Total protein contents were determined by the Bradford method. 30 μ g of proteins were separated by SDS-PAGE under reducing conditions and blotted onto a polyvinylidene difluoride membrane (Millipore). Membranes were probed with specific anti-phospho-ERK1/2 or anti-ERK1/2 antibodies (Cell Signaling Technology) at the dilutions reported by the manufacturer. Signals were revealed

using secondary peroxidase-conjugated antibodies, and the bands visualized by chemoluminescence (Amersham Biosciences). Developed films were scanned using a GS-700 Imaging Densitometer (Bio-Rad) and quantified using Quantity One software (Bio-Rad).

Statistical Analyses—Unpaired Student's *t* tests were done for statistical analyses. Probability values of *p* < 0.01 were considered statistically significant. Experiments were done in triplicate, and data are expressed as means \pm S.E.

RESULTS

HA Quantification and Characterization—As previously described (21), we cultured commercial AoSMCs (Cambrex) in complete-SmGm2 medium (Cambrex) for several population doublings (PD) and consider as “young,” cells with 4 PD after thawing, and as “aged,” cells with 18 PD after thawing. During cell passages, AoSMCs began to show senescence associated β -galactosidase activity, which is considered a typical senescence marker (29), increasing from about 10% in young AoSMCs to about 90% in aged cells indicating a substantial absence of senescence in the cells that we defined as young (21). Moreover, the expression of cyclin p16^{INK4a}, another senescence marker, was significantly higher in aged than in young AoSMCs (21). Moreover, we exclude any dedifferentiation events because a SMC specific marker, α SM actin, and the distribution of actin filaments did not change during cell passages (21).

By FACE analyses, we found that aged cells secrete more HA into the culture medium (Fig. 1A). These findings were confirmed by quantitative HPLC analyses of disaccharides, which measured a significant 20% increase of HA secreted into the culture medium of aged relative to young AoSMCs (Fig. 1B). Moreover, the HPLC analyses also showed that the ratios of disaccharides obtained from chondroitin 4 and 6 sulfate (Δ CS-4S/ Δ CS-6S) decreased during aging from 7.0 \pm 0.5 in young AoSMCs to 5.4 \pm 0.4 in aged cells (data not shown). The relative increase of chondroitin 6-sulfate is known to be linked with the aging process as well as with growth relative to puberty in cartilage (30, 31).

Qualitative assessment of immunofluorescence of cultures showed that HA associated with AoSMCs was higher in aged than in young cells (Fig. 1C). Interestingly, some HA in aged AoSMCs was distributed in spots within cells, as previously reported in mitotic rat aortic SMCs (14, 32).

As the HA molecular weight is an important factor in HA cell responses, we characterized the size distribution of HA released in cell culture medium by young and aged AoSMC cultures with gel filtration. The average HA molecular weight was about 2.2 \times 10⁶ Da in the medium of both young and aged cells (results not shown).

Gene Expression Studies of the HA-metabolizing Enzymes—Quantitative RT-PCR was used to characterize the differences in the expression of HA metabolizing enzymes between young and aged AoSMC cultures. We quantified transcripts coding for the HA synthetic enzymes (HAS1, -2, and -3) and the degrading enzymes (HYAL1, -2, and PH20) using Taqman gene expression assays. In young AoSMCs, HAS3 mRNA is the most abundant transcript for the HA synthetic enzymes, and is

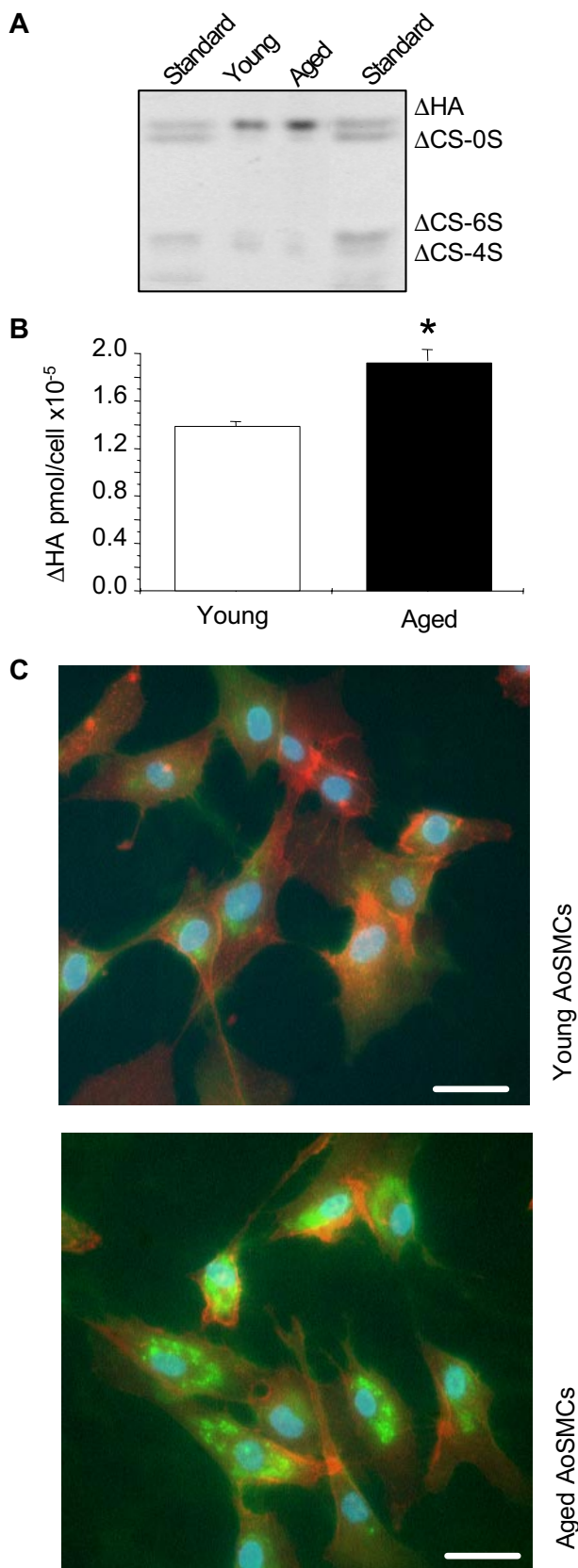


FIGURE 1. A, representative FACE analysis of AMAC-labeled disaccharide of HA (Δ HA), chondroitin 0-sulfated (Δ CS-0S), chondroitin 6-sulfated (Δ CS-6S), and chondroitin 4-sulfated (Δ CS-4S) (standard lanes). AMAC-labeled disaccharides from the GAGs in the culture media conditioned by 10^6 young or aged AoSMCs (Young and Aged lanes, respectively) were prepared as described under "Experimental Procedures." B, HPLC quantification of Δ HA

expressed about 10-fold higher than HAS2 mRNA (Fig. 2A, white bars). HAS2 mRNA, in turn, was expressed about 10-fold higher than HAS1 mRNA. In aged AoSMCs, HAS3 mRNA is expressed only about 1.2-fold higher than HAS2 mRNA, which is expressed about 10-fold higher than HAS1 mRNA (Fig. 2A, black bars). Fig. 2B shows a statistically significant increase of HAS2 mRNA and HAS3 mRNA expression in aged compared with young AoSMCs.

Another protein involved in the onset of atherosclerosis is CD44, the HA receptor (4). This receptor may have a role in vascular cell activation and could mediate inflammatory cell recruitment (5). To verify whether CD44 expression during aging could be altered, we quantified its mRNA level by quantitative RT-PCR and found a statistically significant increase ($\sim 3\times$) in aged AoSMCs (Fig. 2B). Western blot analyses of proteins extracted from young and aged AoSMC cultures confirmed the gene expression data (results not shown). The mRNA expression of the other HA receptor RHAMM did not change during AoSMC aging (Fig. 2E).

We quantified the gene expression of the enzyme that synthesizes the UDP-sugar precursor, UDP-glucuronic acid (UDP-glucose dehydrogenase, UGDH) and found a significantly higher mRNA expression ($\sim 4\times$) in aged AoSMCs (Fig. 2B).

To verify whether our *in vitro* cell aging system represents the gene expression *in vivo*, quantitative RT-PCR was done on human normal aorta RNA prepared from healthy donors of different ages. As a young sample, we used a pool of 5 different fetal aorta RNAs purchased from Invitrogen; as an adult sample we used a pool of 5 different aorta RNAs from donors of >65 years old (Ambion). Fig. 2C highlights the relative ratios for HAS1, -2, and -3 and Fig. 2D shows a statistically significant increase in the expression of mRNA coding for HAS1 enzymes in aged aorta, whereas HAS2 mRNA and HAS3 mRNA appear to be unchanged. Interestingly, in aorta samples, UGDH and CD44 expressions resembled those obtained in the cells aged *in vitro* (Fig. 2, B and D).

Because SMCs in the atherosclerotic lesion change from a contractile to a synthetic phenotype (5), we investigated whether during *in vitro* aging AoSMCs undergo such a phenotypic transition. The expression of critical genes (α -SM actin, VCAM, and ICAM) characteristic of the synthetic phenotype were quantified by quantitative RT-PCR. All three of these genes did not change their expression significantly between young and aged AoSMCs, even though a slight, but not statistically significant, decrease of α -SM actin was found in aged AoSMCs (Fig. 2E). These data indicate that during *in vitro* aging no contractile to synthetic phenotype occurs.

To confirm that the increase of HA in aged AoSMCs could be due to an up-regulation of HAS genes rather than a down-regulation of HYAL genes, we checked the expression of hyaluronidases in AoSMC cultures. HYAL2 mRNA expression was not statistically different in aged compared with young

secreted into the culture medium by young (open bar) and aged (black bar) AoSMCs. The graph represents the means \pm S.E. of three different GAG sample determinations. *, $p < 0.01$ young versus aged. C, immunolocalization of HA (green), CD44 (red), and nuclei (blue) on young and aged AoSMCs. The microphotographs show representative results of different independent experiments. Original magnification $\times 400$. Scale bar is equal to $30 \mu\text{m}$.

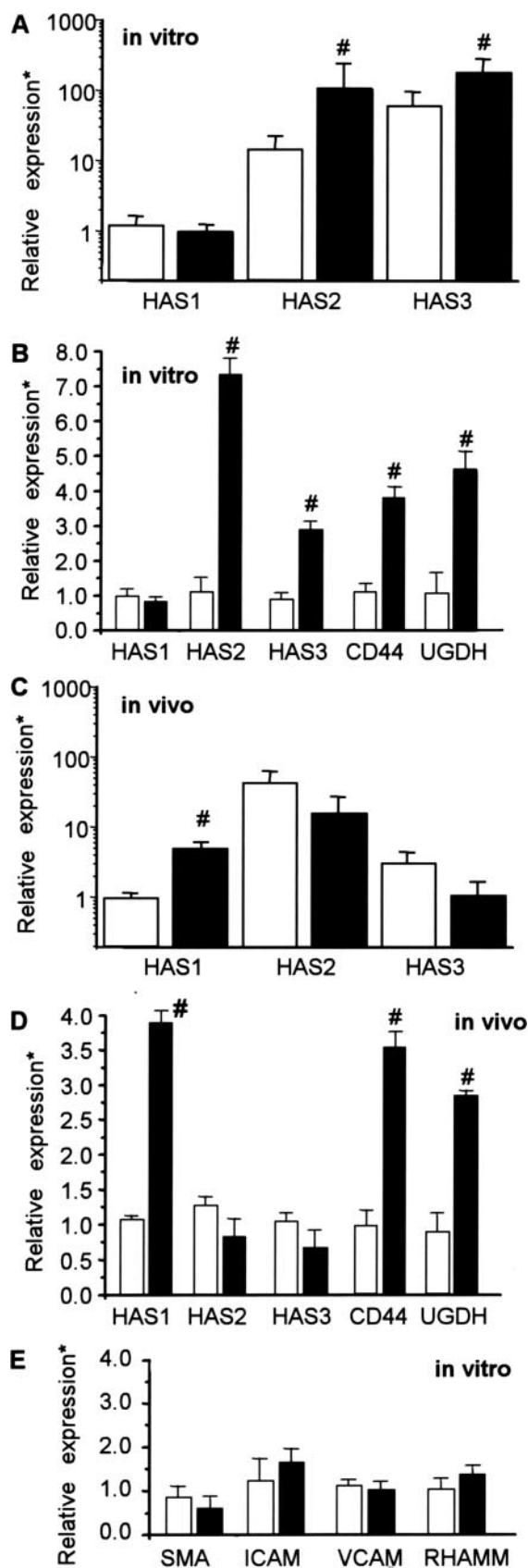


FIGURE 2. A, quantification of the transcripts coding for the HAS enzymes by RT-PCR in young (open bars) and aged (black bars) AoSMCs. The Y axis is in log scale. The results of the relative quantification are calculated using aged HAS1

AoSMCs both *in vitro* and *in vivo* (Fig. 3A). For a control, mRNA coding for PH20, a testis specific hyaluronidase, was quantitated; and, as expected, no signals were found both in young and aged cells (results not shown). HYAL1 mRNA can be alternatively spliced to generate a wild-type functional isoform (HYAL1wt) and five nonfunctional isoform variants (HYAL1v1–5) (25), and the commercial Taqman assays cannot specifically quantify the transcript coding only for the functional enzyme. Hence, we designed two primers that amplified specifically the mRNA for HYAL1wt in a semi quantitative RT-PCR analysis. As shown in Fig. 3B, the band corresponding to HYAL1wt was present only in the BC8701 carcinoma cell line RNA (positive lane), a cell line that possesses hyaluronidase activity in zymography (see Fig. 3, C and D), whereas neither young nor aged AoSMCs express the mRNA coding for the functional enzyme.

The human genome possesses other HYAL genes coding for HYAL3, whose function is still unknown, and HYAL4, a pseudogene transcribed but not translated in humans (34). We did not observe any bands corresponding to HYAL3 mRNA or HYAL4 mRNA in RT-PCR experiments indicating that, if they were expressed, their transcript levels were below the detection limit of RT-PCR (Fig. 3E).

Hyaluronidase zymography at pH 3.5 (Fig. 3C) and electrophoretic analysis of hyaluronidase activity on soluble commercial HA (27) (Fig. 3D) clearly indicate that no hyaluronidase activity can be detected in either the conditioned culture media or in cell extracts of young and aged AoSMC cultures. Similar results were obtained when the hyaluronidase zymography was done at pH 5 (results not shown). These results suggest that the age related HA accumulation is due to an up-regulation of HA synthetic enzymes (*i.e.* HAS2 and 3) rather than a down-regulation of degrading enzymes.

AoSMCs Behavior during Aging—One of the most precocious events during the onset of atherosclerosis or restenosis is SMC migration toward the intima layer. As it is known that CD44 promotes atherosclerosis (5), we focused our attention on AoSMC migration during aging in relation to HA, CD44 and the effects of CD44 on the MAP kinase ERK1/2 phosphorylation signaling pathway (35). We hypothesized that the high CD44 expression in aged cells could mediate higher levels of phosphorylated ERK1/2 protein. Phosphorylation of p44/42 MAP kinase (ERK1/2) at residues Thr202 and Tyr204 activates the protein, which triggers several cellular events including

expression as reference. B, quantification of the transcripts coding for the HAS enzymes, CD44 and UGDH by RT-PCR in young (open bars) and aged (black bars) AoSMCs. The mRNA expression of each gene in young samples is used as reference, the lowest value of five different determinations of young samples was set to one, and the S.E. is shown on each bar. C, quantification of the transcripts coding for the HAS enzymes in fetal aorta (open bars) and adult aorta (black bars). The Y axis is in log scale. The results of the relative quantification are calculated using aged HAS1 expression as reference. D, quantification of the transcripts coding for the HAS enzymes, CD44 and UGDH by RT-PCR by using cDNA derived from fetal (open bars) and adult aorta (black bars) total RNA. The expression of each gene in young samples is used as reference as reported above. E, quantification of the transcripts coding for α -SM actin (SMA), ICAM, VCAM, and RHAMM by RT-PCR in young and aged AoSMCs. The expression of each gene in young samples is used as reference as reported above. Relative expression is expressed in arbitrary units. #, $p < 0.01$ young versus aged. Data represent mean \pm S.E. of three different experiments. Asterisks indicate arbitrary units.

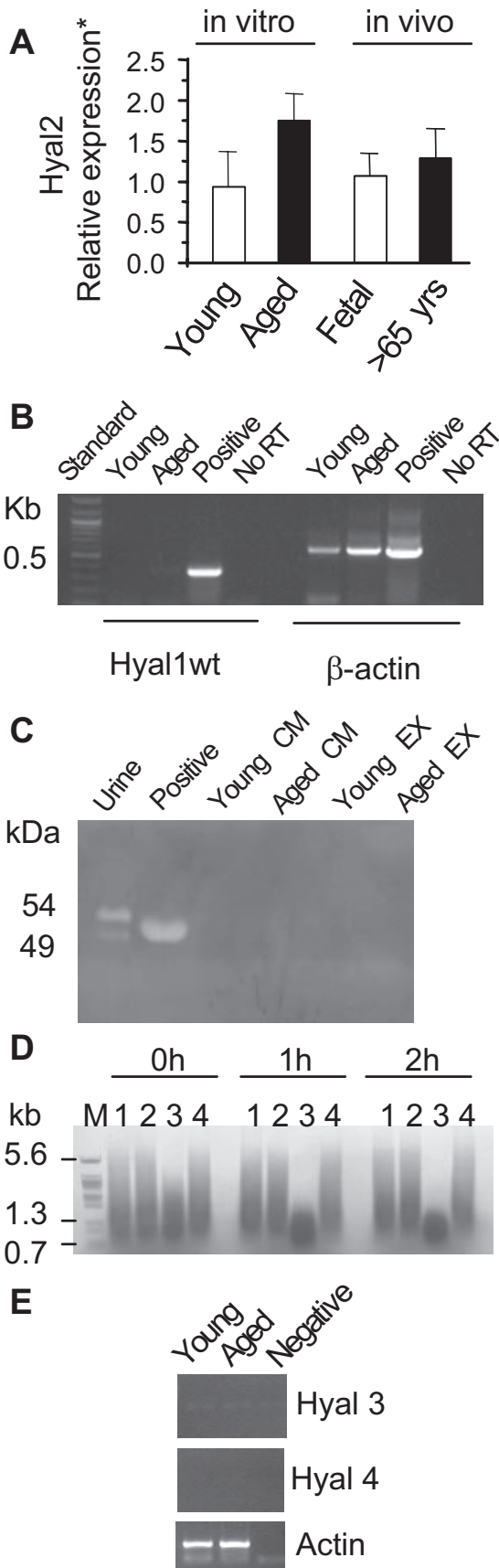


FIGURE 3. A, quantification of the transcripts coding for HYAL2 enzyme by RT-PCR in young AoSMCs or fetal aorta (open bars) and aged AoSMCs or adult aorta (black bars). The expression of HYAL2 gene in young or fetal samples is

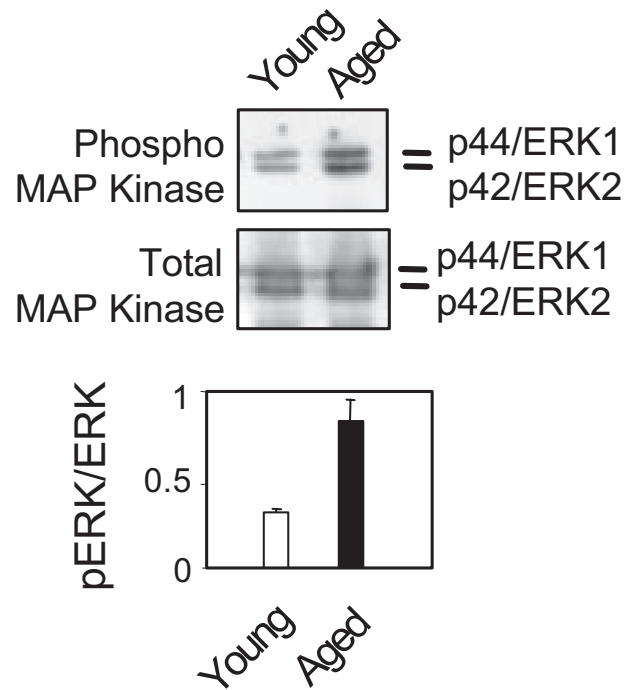


FIGURE 4. Western blot analysis to detect ERK1/2 phosphorylation in young and aged AoSMCs (upper panels). 30 μ g of proteins were loaded in each lane and were prepared from 80% confluent cultures of young and aged AoSMCs grown in SmGm2 complete culture medium supplemented with 5% FBS. Anti-phosphorylated ERK1/2 antibody was used to detect the active MAP kinase. After stripping, the membrane was probed with anti-total ERK1/2 to visualize the total amount of MAP kinase. The photograph shows representative results of three independent experiments. The lower panel shows densitometric analyses of Western blot bands.

cell migration. Western blot analysis of protein extracts from young and aged AoSMC cultures showed higher levels of phosphorylated ERK1/2 protein in aged cells (Fig. 4). We repeated the experiment several times and always found about a 2-fold increase of ERK1/2 phosphorylation in aged cells compared with young cells. By using a Transwell system, we assessed the migration of young and aged AoSMCs as previously described (21). Without covering the Tran-

used as reference as described in the Fig. 2 legend. Asterisk indicates arbitrary units. B, semiquantitative RT-PCR analysis of young and aged AoSMCs total RNA (young and aged lanes, respectively) using primers that amplified only the catalytically active isoform of HYAL1. As a control, β actin was also amplified. Total RNA from BC8701 cells was used as a positive control (positive lane). Negative controls were done by amplifying young and aged total RNA without the reverse transcription step (no RT lanes). C, hyaluronidase zymography done on 10 \times concentrated young or aged AoSMCs conditioned culture medium (Young CM and Aged CM lanes, respectively) and on 50 μ g of proteins extracted from young or aged AoSMCs (young extract and aged extract lanes, respectively). As controls, concentrated human urine (urine lane) and the conditioned cell culture medium of BC8701 cell line (positive lane) were loaded in the gel. The gel was incubated at pH 3.5, and the bands were visualized by Alcian Blue staining. The photograph shows a representative result of several independent experiments. D, hyaluronidase activity in 30 μ g of proteins extracted from young AoSMCs (lane 1), aged AoSMCs (lane 2), BC8701 (lane 3, positive controls) on commercial HA at pH 5 at the indicated incubation times. Lanes 4 contain no protein extracts (negative controls). Lane M contains λ DNA digested with BstEI as a molecular marker. HA in the agarose gel is visualized by Stains-All staining. E, semiquantitative RT-PCR on cDNA synthesized from young and aged AoSMCs total RNA. Primers were used to amplify Hyal3 and Hyal4. Positive controls were done detecting cytoskeletal actin.

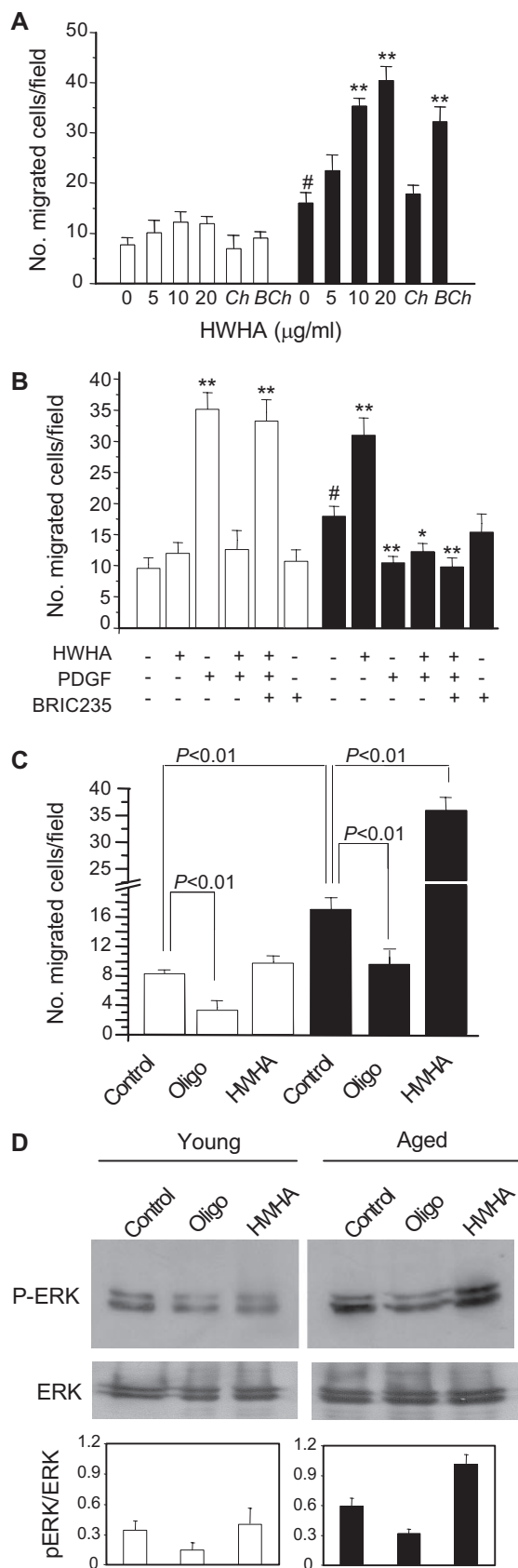


FIGURE 5. A, effect of different concentrations of HWA on the migration of young and aged AoSMCs using a Transwell apparatus. 10 μ g/ml of chondroitinase ABC digested HWA were added in *ch* sample; 10 μ g/ml of HWA treated with boiled chondroitinase ABC were added in *BCh* sample. B, effects

swell with any matrix molecules, aged AoSMCs showed higher migratory capability than young AoSMCs (Fig. 5, A and B and Fig. 6A).

To assess the effect of HA on AoSMC migration, we added different concentrations of high molecular weight HA (HWA) (Healon, average MW \sim 4000 kDa) to the lower chamber of the Transwell. Young AoSMCs did not change motility whereas HWA stimulated aged AoSMC migration in a dose-dependent manner (Fig. 5A). A statistically significant effect was seen at 10 μ g/ml HWA, and this concentration was used for further experiments. To control the specificity of HA effects on migration, chondroitinase ABC-digested HWA was added to AoSMCs. The treatment with digested HWA did not alter the migratory capabilities of the cells compared with cells tested in the absence of HWA. On the other hand, control experiments using HWA treated with heat inactivated chondroitinase ABC showed the same induction of cell migration as obtained with cells in the presence of HWA (Fig. 5A). These controls indicate that the alteration in migration of the aged AoSMCs is specific for the HWA and not due to a contaminant.

PDGF-BB, a standard molecule used to induce cell migration (36), at 10 ng/ml, induced a statistically significant increase in migration of young AoSMCs whereas aged AoSMCs showed a significant reduction of motility (Fig. 5B). The simultaneous treatment of HWA and PDGF-BB did not change migration of young AoSMCs compared with untreated cells, whereas they significantly reduced the motility of aged AoSMCs. Interestingly, the treatment with BRIC235, a monoclonal blocking antibody against CD44 that inhibits HA-CD44 binding (37), restored the migration level induced by PDGF-BB in young AoSMCs. On the other hand, the BRIC235 treatment significantly decreased the migration of aged AoSMCs (Fig. 5B). Similar effects were observed also using the A3D8 anti-CD44 monoclonal antibody that did not inhibit specifically HA-CD44 binding (38) (data not shown). An isotype control monoclonal antibody did not alter migration of either young or aged AoSMCs (data not shown). Interestingly, without any treatment, a statistically significant increase of cell motility of aged compared with young AoSMCs was always observed (Fig. 5, A-C).

of HWA (10 μ g/ml), PDGF-BB (10 ng/ml), and anti-CD44 blocking antibody (BRIC235, 5 μ g/ml) on the migration of young and aged AoSMCs using a Transwell apparatus. C, effects of PBS (control) or 10 μ g/ml 34-mer HA oligosaccharide (oligo) or 10 μ g/ml HWA (HWA) on the migration of young and aged AoSMCs using a Transwell apparatus. In all these experiments, AoSMCs were seeded in the upper chamber of the apparatus and treated by adding test reagents in the lower chamber of the Transwell. After 6 h of incubation at 37 $^{\circ}$ C, migrated cells were counted in six independent microscope fields. Y axis represents the number of migrated cells/field. White bars represent young AoSMC samples, and black bars represent aged AoSMC samples. Data represent mean \pm S.E. of three independent experiments. D, Western blot analysis of phosphorylation of ERK1/2 proteins in young and aged AoSMCs treated with PBS (control) or 10 μ g/ml 34-mer HA oligosaccharide (oligo) or 10 μ g/ml HWA (HWA) using anti-phospho-ERK1/2 to detect the active MAP kinase. After stripping, the membrane was probed with anti-total-ERK1/2 to visualize the total amount of MAP kinase (upper panels). The photographs show representative results of three independent panels. Densitometric analyses of Western blot bands (lower panel). #, $p < 0.01$ untreated young versus untreated aged cells, **, $p < 0.01$ untreated versus treated samples.

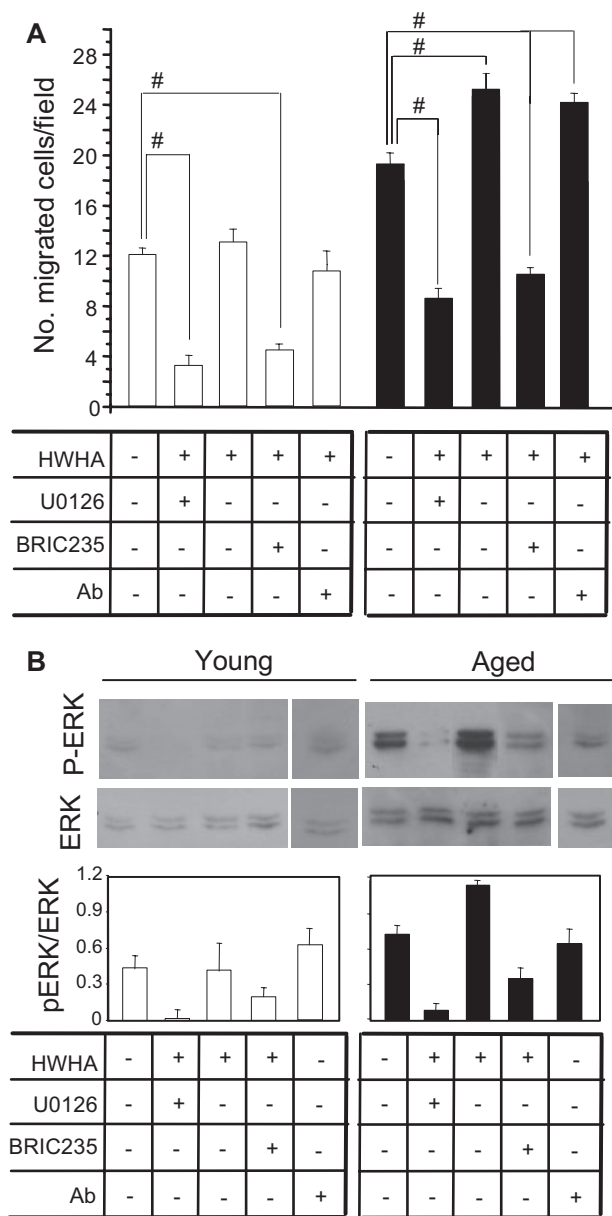


FIGURE 6. *A*, migration of young and aged AoSMCs using a Transwell apparatus. AoSMCs were seeded in the upper chamber of the apparatus and treated with or without 10 $\mu\text{g/ml}$ HWHA, 15 μM of U0126, 15 $\mu\text{g/ml}$ of monoclonal anti CD44 antibody (BRIC235) or 15 $\mu\text{g/ml}$ of a control isotype monoclonal antibody (Ab) as described in the Fig. 5 legend. White bars represent young AoSMC samples, and black bars represent aged AoSMC samples. Data represent mean \pm S.E. of three independent experiments. #, $p < 0.01$ untreated versus treated samples. *B*, Western blot analyses of phosphorylation of ERK1/2 proteins in young and aged AoSMCs treated with or without 10 $\mu\text{g/ml}$ HWHA, 15 μM of U0126, 15 $\mu\text{g/ml}$ of monoclonal anti-CD44 antibody (BRIC235) or 15 $\mu\text{g/ml}$ of a control isotype monoclonal antibody. The photographs show representative results of three independent experiments. Densitometric analyses of Western blots bands (lower panel).

As HA of different molecular weight can modify cell migration (38), we added a 34-mer HA oligosaccharide (a kind gift from Akira Asari) or HWHA to the Transwell. As shown in Fig. 5C, 34-mer oligosaccharide reduced the migration of both young and aged AoSMCs. In contrast, as described above, HWHA did not significantly change the migration of young cells, but increased the migration of aged AoSMCs about 2-fold.

The migratory capability of the cells could depend upon phosphorylation of ERK1/2 protein. Thirty minutes treatment of young and aged AoSMCs with 10 $\mu\text{g/ml}$ of 34-mer oligosaccharide or 10 $\mu\text{g/ml}$ of HWHA altered ERK1/2 phosphorylation (Fig. 5D). In young AoSMCs, the 34-mer oligosaccharide caused a decrease in ERK1/2 phosphorylation whereas HWHA did not modify ERK1/2 phosphorylation. Similarly, 34-mer oligosaccharide caused a decrease in ERK1/2 phosphorylation in aged cells, whereas, interestingly, the treatment of aged AoSMCs with HWHA induced a marked increase of phosphorylation of ERK1/2 (Fig. 5D).

As the expression of CD44 varied during cell aging, we tested whether migration that is modulated by HA and ERK1/2 phosphorylation could be due to CD44 signaling. As shown in Fig. 6, *A* and *B*, by adding U0126, an inhibitor of ERK1/2 phosphorylation, at a final concentration of 15 μM , there was a clear reduction of cell migration and ERK1/2 phosphorylation both in young and aged AoSMCs. Similarly, adding the BRIC235 anti-CD44 blocking antibody reduced ERK1/2 phosphorylation and migration. Similar results were obtained using the A3D8 antibody (results not shown). As a control, adding an isotype-matched antibody did not induce any difference in migration or in ERK1/2 phosphorylation. Interestingly, U0126 and anti-CD44 blocking antibody inhibited ERK1/2 phosphorylation in both young and aged AoSMCs (Fig. 6B). In young AoSMCs, the addition of HWHA did not significantly change either migration or ERK1/2 phosphorylation.

DISCUSSION

There is a clear correlation between aging and the probability for onset of cardiovascular diseases (20). For this reason, we studied HA metabolism in AoSMCs during *in vitro* aging to verify whether they could modify their matrix environment with aging and acquire a more susceptible phenotype that could promote vascular diseases. It is well known that cell behavior depends upon their surroundings through physical contacts with other cells or ECM. We focused our attention on human AoSMCs as this cell type is involved in neointima formation. In response to incompletely known stimuli or injuries, AoSMCs proliferate and migrate from the media to the intima layer during early development of vascular disease. We established an *in vitro* aging model based on cell senescence. It was reported that during aging the percentage of senescent cells also increased at the vascular level (39). In our previous work, we demonstrated that the cells that we defined as "young" did not express any marker of senescence whereas the cells that we defined as "aged" were positive for senescent associated β -galactosidase staining and for p16^{INK4A} cyclin (21). Moreover, as cells were cultivated for a long time and many passages, we excluded any dedifferentiation events by quantifying and studying the cellular distribution of SM actin filaments, which did not change with aging *in vitro* (21).

Comparing young and aged AoSMCs, we found a significant increase of HA released into the culture medium of aged AoSMCs. Moreover, the cellular distribution revealed an increase in HA inside the aged cells similar to that observed in dividing SMCs by other investigators (14, 32). As the amount of each cellular component is determined by the balance between

Hyaluronan during Smooth Muscle Cell Aging

its synthesis and degradation, we quantified the relative expression of anabolic and catabolic HA enzymes by quantitative RT-PCR and found that the HA accumulation during aging is likely to be the result of increased expression of synthetic enzymes rather than a down-regulation of degrading enzymes.

We also compared the gene expression obtained in the *in vitro* model with RNA from human donors. The gene expression experiments carried out *in vivo* on fetal and adult aortic tissue showed an increase of UGDH and CD44 in adult samples, showing the same findings that we obtained in *in vitro* experiments comparing young and aged AoSMCs. We previously demonstrated that high levels of UGDH, the enzyme that catalyzes the oxidation of UDP-glucose to UDP-glucuronic acid, induced an increase of HA synthesis (40). Therefore, the increase of UGDH during aging is in agreement with the accumulation of HA in aged cells.

During *in vivo* aging we found an up-regulation of HAS1 rather than HAS2 and HAS3. Although *in vivo* the up-regulated gene was a different enzyme of the HAS family, this result confirms that the expression of HA synthetic enzymes increased both *in vivo* and *in vitro* aging. Nevertheless, the different isoform expression may reflect that the simpler *in vitro* model differs from the *in vivo* complex environment inducing cells to express a different synthase enzyme. Moreover, it is to be considered that young cells for the *in vitro* data came from a young, but mature donor whereas RNA for the *in vivo* experiments came from fetal tissues. Previous work showed that HAS1 together with HAS2 are the more abundant HAS isoforms expressed in saphenous vein, whereas SMCs isolated from the same vessel expressed mainly HAS2 and HAS3 (41). Even if a clear correlation is not reported in the literature between age and GAG content in the ECM of vessels (30), other studies reported an age increase of HA in aorta bifurcation (42) and in cerebral arteries (43). During rat aging, a significant increase of HA is observed at the vascular level (44). In a mouse model of Hutchinson-Gilford progeria syndrome, a pathology characterized by a precocious senility, there is a clear HA accumulation in the aorta (45). This information supports the hypothesis that during aorta aging an accumulation of HA occurs.

In our study, HA accumulation is not dependent on hyaluronidase activity. We were not able to detect any hyaluronidase activity in either the conditioned media or in cell extracts. RT-PCR and zymography demonstrated that both young and aged AoSMCs did not express mRNA for HYAL1wt nor for HYAL3 and 4. Moreover, HYAL2 mRNA expressions in young and aged AoSMCs and in fetal and aged aorta were not statistically different. Although HYAL2 was reported to have a hyaluronidase activity (27, 34), several researchers were not able to detect hyaluronidase activity even after HYAL2 cDNA transfections (47). These data suggest that this protein could possess a different function, such as a virus receptor (46). Another possibility to explain the lack of hyaluronidase activity is that HYAL2 could require an activation process or possesses a cellular inhibitor that prevents its function. It could also be noted that this enzyme may generate large fragments of HA that would not be detected by the methods used.

As CD44 and RHAMM can influence SMC behavior (6), we found that only the expression of CD44 was significantly

increased in both aged cells and adult aorta RNA. The accumulation of HA in the ECM and the CD44 overexpression suggest that during aging a modification in the expression of HA synthetic and signaling genes can occur that could induce AoSMCs to be more proliferative, as Cuff *et al.* (5) demonstrated in 2001, and more migratory. Other researchers reported that CD44-modulated cell motility may have a role in several pathologies (48). The migration assay showed that aged cells increased their migration capacity, and CD44 is expressed more in aged cells. Nevertheless, the size of the HA appears critical for this modulation as low molecular weight HA had different effects on migration than high molecular weight HA.

Our data also support the hypothesis that CD44 clusterization is a crucial condition to obtain efficient transduction signals (35). The phosphorylation of MAP kinase ERK1/2, a protein in the CD44 internalization pathway that includes also PI3K, ERB, and AKT (49), is clearly involved in cell motility (50). In our experimental model, we found that ERK1/2 phosphorylation is triggered by CD44 and large molecular weight HA interactions. Therefore, increased ERK1/2 phosphorylation in aged AoSMCs combined with increased migration capacity likely depends on both augmented HA synthesis and higher expression of CD44 since treatment with HA oligosaccharide of 34-mer and the CD44 blocking antibody reduced both ERK1/2 phosphorylation and cell migration. Interestingly, the A3D8 anti CD44 antibody that did not block HA binding to CD44, inhibited cell migration in our model and in other models (12, 51), probably by preventing CD44 conformation changes induced by HA binding. However, in other systems it did not affect migration (53). Other pathways involving VCAM and ICAM proteins could control the migratory capability of AoSMCs. However, there were no differences in VCAM and ICAM mRNA expression between young and aged AoSMCs. Therefore, HA can control AoSMC migration through interactions with CD44 and subsequent ERK phosphorylation.

These findings correlate well with the observation obtained *in vivo* that the response of vessel injury is much greater in vessels of older animals (54). The different behavior between young and aged vessels could be ascribed to a different response to signaling molecules as previously described for bFGF and PDGF (55).

We found that PDGF-BB enhanced young AoSMC migration, but it reduced aged AoSMC motility and that HWHA strongly modulated the responses. In young AoSMCs, HWHA inhibited PDGF-BB stimulated migration, and this effect could be reversed by blocking HA-CD44 interactions, similar to results recently obtained by Li *et al.* (46). They reported that the induced PDGF-BB migration in fibroblasts was reduced by HA through a mechanism involving PDGFR- β phosphorylation. On the other hand, in the case of aged AoSMCs, PDGF-BB reduced cell migration induced by HWHA, and this effect was independent of HA-CD44 interactions as shown by blocking experiments using anti-CD44 antibodies. Further, quantitative RT-PCR showed that young AoSMCs expressed 2-fold more PDGFR β than PDGFR α whereas, in aged AoSMCs, the ratio was inverted (results not shown). This indicates that the aging of AoSMCs may alter the PDGF receptor chain ratio on the cell membrane.

The high migratory capability of aged AoSMCs fits well with their high expression of CD44. However, it is not clear whether cells extracted from aged animals have higher migration rates than cells extracted from young animals. Controversial results were obtained from SMCs prepared from young and aged human or animal models. Aged human SMCs showed a limited migration (33) whereas aged rat SMCs showed an increase of migration (52). However, it is possible that the microenvironment surrounding cells influences the cell behavior. For example, we previously reported that the migration of aged AoSMCs on a gelatin rich matrix was different due to differences in metalloproteinase 2 activity (20). The absence of an external matrix in the model used in the experiments described in this report highlights the specific role of HA in AoSMC migration.

In conclusion we demonstrated that during *in vitro* aging, AoSMCs accumulate HA by increasing HA synthetic enzymes. Moreover, we provided evidence that HWAHA induces migration of aged AoSMCs probably through a CD44-mediated pathway by controlling the activity of MAP kinase ERK1/2.

Acknowledgments—We thank Dr. Akira Asari (Glycoscience Laboratories, Inc.) for the 34-mer HA oligosaccharide, Dr. Frances Spring (National Blood Service, UK) for Bric235 monoclonal antibodies, Dr. Raffaella Cinquetti for aorta RNAs. The authors gratefully acknowledge the “Centro Grandi Attrezzature per la Ricerca Biomedica” Università degli Studi dell’Insubria, for the instrument facility.

REFERENCES

- Toole, B. P., Wight, T. N., and Tammi, M. I. (2002) *J. Biol. Chem.* **277**, 4593–4596
- Itano, N., Sawai, T., Yoshida, M., Lenas, P., Yamada, Y., Imagawa, M., Shinomura, T., Hamaguchi, M., Yoshida, Y., Ohnuki, Y., Miyauchi, S., Spicer, A. P., McDonald, J. A., and Kimata, K. (1999) *J. Biol. Chem.* **274**, 25085–25092
- Tien, J. Y., and Spicer, A. P. (2005) *Dev. Dyn.* **233**, 130–141
- Turley, E. A., Noble, P. W., and Bourguignon, L. Y. W. (2002) *J. Biol. Chem.* **277**, 4589–4592
- Cuff, C. A., Kothapalli, D., Azonobi, I., Chun, S., Zhang, Y., Belkin, R., Yeh, C., Secreto, A., Assoian, R. K., Rader, D. J., and Pure, E. (2001) *J. Clin. Invest.* **108**, 1031–1040
- Nedvetzki, S., Gonen, E., Assayag, N., Reich, R., Williams, R. O., Thurmond, R. L., Huang, J., Neudecker, B. A., Wang, F., Turley, E. A., and Naor, D. (2004) *Proc. Natl. Acad. Sci. U. S. A.* **101**, 18081–18086
- Johnson, L. A., Prevo, R., Clasper, S., and Jackson, D. G. (2007) *J. Biol. Chem.* **282**, 33671–33680
- Harris, E. N., Weigel, J. A., and Weigel, P. H. (2004) *J. Biol. Chem.* **279**, 36201–36209
- Harris, E. N., Kyosseva, S. V., Weigel, J. A., and Weigel, P. H. (2007) *J. Biol. Chem.* **282**, 2785–2777
- Termeer, C., Benedix, F., Sleeman, J., Fieber, C., Voith, U., Ahrens, T., Miyake, K., Freudenberg, M., Galanos, C., and Simon, J. C. (2002) *J. Exp. Med.* **195**, 99–111
- Jiang, D., Liang, J., Fan, J., Yu, S., Chen, S., Luo, Y., Prestwich, G. D., Mascarenhas, M. M., Garg, H. G., Quinn, D. A., Homer, R. J., Goldstein, D. R., Bucala, R., Lee, P. J., Medzhitov, R., and Noble, P. W. (2005) *Nat. Med.* **11**, 1173–1179
- de la Motte, C. A., Hascall, V. C., Drazba, J., Bandyopadhyay, S. K., and Strong, S. A. (2003) *Am. J. Pathol.* **163**, 121–133
- Majors, A. K., Austin, R. C., de la Motte, C. A., Pyeritz, R. E., Hascall, V. C., Kessler, S. P., Sen, G., and Strong, S. A. (2003) *J. Biol. Chem.* **278**, 47223–47231
- Hascall, V. C., Majors, A. K., De La Motte, C. A., Evanko, S. P., Wang, A., Drazba, J. A., Strong, S. A., and Wight, T. N. (2004) *Biochim. Biophys. Acta* **1673**, 3–12
- Wang, A., and Hascall, V. C. (2004) *J. Biol. Chem.* **279**, 10279–10285
- Heldin, P. (2003) *Braz. J. Med. Biol. Res.* **36**, 967–973
- Riessen, R., Wight, T. N., Pastore, C., Henley, C., and Isner, J. M. (1996) *Circulation* **93**, 1141–1147
- Tzircotis, G., Thorne, R. F., and Isacke, C. M. (2005) *J. Cell Sci.* **118**, 5119–5128
- Chai, S., Chai, Q., Danielsen, C. C., Hjorth, P., Nyengaard, J. R., Ledet, T., Yamaguchi, Y., Rasmussen, L. M., and Wogensen, L. (2005) *Circ. Res.* **96**, 583–591
- Spagnoli, L. G., Orlandi, A., Mauriello, A., Santeusano, G., Angelis, C., Lucreziotti, R., and Ramacci, M. T. (1991) *Atherosclerosis* **89**, 11–24
- Vigetti, D., Moretto, P., Viola, M., Genasetti, A., Rizzi, M., Karousou, E., Pallotti, F., De Luca, G., and Passi, A. (2006) *FASEB J.* **20**, 1118–1130
- Karousou, E. G., Militopoulou, M., Porta, G., De Luca, G., Hascall, V. C., and Passi, A. (2004) *Electrophoresis* **25**, 2919–2925
- Raio, L., Cromi, A., Grezzi, F., Passi, A., Karousou, E., Viola, M., Vigetti, D., De Luca, G., and Bolis, P. (2005) *Matrix Biol.* **24**, 166–174
- Winer, J., Jung, C. K., Shackel, I., and Williams, P. M. (1999) *Anal. Biochem.* **270**, 41–49
- Lokeshwar, V. B., Schroeder, G. L., Carey, R. I., Soloway, M. S., and Iida, N. (2002) *J. Biol. Chem.* **277**, 33654–33663
- Miura, R. O., Yamagata, S., Miura, Y., Harada, T., and Yamagata, T. (1995) *Anal. Biochem.* **225**, 333–340
- Lepperdinger, G., Strobl, B., and Kreil, G. (1998) *J. Biol. Chem.* **273**, 22466–22470
- Tawada, A., Masa, T., Oonuki, Y., Watanabe, A., Matsuzaki, Y., and Asari, A. (2002) *Glycobiology* **12**, 421–426
- Dimri, G. P., Lee, X., Basile, G., Acosta, M., Scott, G., Roskelley, C., Medrano, E. E., Linskens, M., Rubelj, I., and Pereira-Smith, O. (1995) *Proc. Natl. Acad. Sci. U. S. A.* **92**, 9363–9367
- Tovar, A. M., Cesar, D. C., Leta, G. C., and Mourao, P. A. (1998) *Arterioscler. Thromb. Vasc. Biol.* **18**, 604–614
- Plaas, A. H., Wong-Palms, S., Roughley, P. J., Midura, R. J., and Hascall, V. C. (1997) *J. Biol. Chem.* **272**, 20603–20610
- Evanko, S. P., and Wight, T. N. (1999) *J. Histochem. Cytochem.* **47**, 1331–1342
- Ruiz-Torres, A., Lozano, R., Melon, J., and Carraro, R. (2003) *J. Gerontol. A Biol. Sci. Med. Sci.* **58**, B1074–B1077
- Harada, H., and Takahashi, M. (2007) *J. Biol. Chem.* **282**, 5597–5607
- Toole, B. P. (2004) *Nat. Rev. Cancer.* **4**, 528–539
- Arita, Y., Kihara, S., Ouchi, N., Maeda, K., Kuriyama, H., Okamoto, Y., Kumada, M., Hotta, K., Nishida, M., Takahashi, M., Nakamura, T., Shimomura, I., Muraguchi, M., Ohmoto, Y., Funahashi, T., and Matsuzawa, Y. (2002) *Circulation* **105**, 2893–2898
- Liao, H. X., Lee, D. M., Leveque, M. C., and Haynes, B. F. (1995) *J. Immunol.* **155**, 3938–3945
- Slevin, M., Kumar, S., and Gaffney, J. (2002) *J. Biol. Chem.* **277**, 41046–41059
- Martin, G. M., Ogburn, C. E., and Wight, T. N. (1983) *Am. J. Pathol.* **110**, 236–245
- Vigetti, D., Ori, M., Viola, M., Genasetti, A., Karousou, E., Rizzi, M., Pallotti, F., Nardi, I., Hascall, V. C., De Luca, G., and Passi, A. (2006) *J. Biol. Chem.* **281**, 8254–8263
- van den Boom, M., Sarbia, M., von Wnuck Lipinski, K., Mann, P., Meyer-Kirchthar, J., Rauch, B. H., Grabitz, K., Levkau, B., Schror, K., and Fischer, J. W. (2006) *Circ. Res.* **98**, 36–44
- Stuhlsatz, H. W., Loffler, H., Mohanaradhakrishnan, V., Cosma, S., and Greiling, H. (1982) *J. Clin. Chem. Clin. Biochem.* **20**, 713–721
- Murata, K., and Yokoyama, Y. (1989) *Atherosclerosis* **78**, 69–79
- Chajara, A., Delpech, B., Courel, M. N., Leroy, M., Basuyau, J. P., and Levesque, H. (1998) *Atherosclerosis* **138**, 53–64
- Varga, R., Eriksson, M., Erdos, M. R., Olive, M., Harten, I., Kolodgie, F., Capell, B. C., Cheng, J., Faddah, D., Perkins, S., Avallone, H., San, H., Qu, X., Ganesh, S., Gordon, L. B., Virmani, R., Wight, T. N., Nabel, E. G., and Collins, F. S. (2006) *Proc. Natl. Acad. Sci. U. S. A.* **103**, 3250–3255
- Li, L., Heldin, C. H., and Heldin, P. (2006) *J. Biol. Chem.* **281**, 26512–26519
- Rai, S. K., Duh, F. M., Vigdorovich, V., Danilkovitch-Miagkova, A., Lerman,

Hyaluronan during Smooth Muscle Cell Aging

- M. I., and Miller, A. D. (2001) *Proc. Natl. Acad. Sci. U. S. A.* **98**, 4443–4448
48. Isacke, C. M., and Yarwood, H. (2002) *Int. J. Biochem. Cell Biol.* **34**, 718–721
49. Bourguignon, L. Y., Gilad, E., Rothman, K., and Peyrollier, K. (2005) *J. Biol. Chem.* **280**, 11961–11972
50. Cox, B. D., Natarajan, M., Stettner, M. R., and Gladson, C. L. (2006) *J. Cell. Biochem.* **99**, 35–52
51. Clark, R. A. F., Lin, F., Greiling, D., An, J., and Couchman, J. R. (2004) *J. Investig. Dermatol.* **122**, 266–277
52. Li, Z., Cheng, H., Lederer, W. J., Froehlich, J., and Lakatta, E. G. (1997) *Exp. Mol. Pathol.* **64**, 1–11
53. Kitayama, J., Juji, T., Atomi, Y., Kuroda, A., Muto, T., Kobayashi, M., Mitsui, Y., and Minami, M. (1993) *J. Immunol.* **151**, 1663–1672
54. Hariri, R. J., Alonso, D. R., Hajjar, D. P., Coletti, D., and Weksler, M. E. (1986) *J. Exp. Med.* **164**, 1171–1178
55. Lundberg, M. S., and Crow, M. T. (1999) *Exp. Gerontol.* **34**, 549–557

